



FYS3150: Computational Physics I

Project 4

Studies of Phase Transitions in Magnetic Systems Using the Square Lattice Ising Model and the Metropolis Algorithm

Nicolai Haug*

November 21, 2018

Abstract

In this project the square lattice Ising model for a magnetic system with ferromagnetic ordering was used to simulate phase transitions, with the aim to determine the Curie temperature T_C . The Metropolis algorithm was used to calculate the Ising model estimations with periodic boundary conditions. In simulations with various finite lattices of size $L \times L$, specifically $L = 40, 60, 100, 160$, the Curie temperature was extracted with finite scaling relations as $k_B T_C / J \approx 2.268$, where J and k_B is a coupling and the Boltzmann constant, respectively. This corresponds well with the exact result, $k_B T_C / J = 2 / \ln(1 + \sqrt{2}) \approx 2.269$ provided by Onsager [1].

*This project was embarked on as a collaborative effort between Lasse Braseth, Nicolai Haug, and Kristian Wold. Hence, our individual reports have a strong resemblance in both presentation and content. In particular, figures and tables with corresponding captions are nearly, or in some cases entirely, identical.

Contents

1	Introduction	1
2	Theory	2
2.1	A Short Review of Statistical Mechanics	2
2.2	The Ising Model	3
2.3	Periodic Boundary Conditions	4
2.4	Analytical Expressions of the Ising Model	5
2.5	Second Order Phase Transitions in the Ising Model	6
2.6	The Metropolis Algorithm	7
3	Method	9
3.1	Implementing the Metropolis Algorithm	9
3.2	Verifying the Implementation	11
3.3	Equilibrium for Ordered and Disordered Initial State	11
3.4	Number of Accepted States	11
3.5	Probability Distribution	11
3.6	Studies of Phase Transitions	12
3.7	Parallelization Speedup	12
3.8	Extracting the Curie Temperature	12
4	Results	13
4.1	Implementing the Metropolis Algorithm	13
4.2	Verifying the Implementation	13
4.3	Equilibrium for Ordered and Disordered Initial State	15
4.4	Number of Accepted States	17
4.5	Probability Distribution	18
4.6	Studies of Phase Transitions	19
4.7	Parallelization Speedup	21
4.8	Extracting the Curie Temperature	22
5	Discussion	23
5.1	Implementing the Metropolis Algorithm	23
5.2	Verifying the Implementation	23
5.3	Equilibrium for Ordered and Disordered Initial State	23
5.4	Number of Accepted States	24
5.5	Probability Distribution	24
5.6	Studies of Phase Transitions	25
5.7	Parallelization Speedup	25
5.8	Extracting the Curie Temperature	26
6	Conclusion	26
7	Future Work	26

1 Introduction

In statistical mechanics, the Ising model is a model of interacting magnetic dipole moments of atomic spins. The spins are arranged in a lattice, allowing each spin to interact with its neighbors. The two dimensional square lattice Ising model exhibits a phase transition from a magnetic phase (a system with finite magnetic moment) to a phase with zero magnetization at a given critical temperature, called the Curie temperature.

In this project, the aim is to study the phase transitions shown by the Ising model with ferromagnetic ordering, as well as the Ising model itself. This will be done by the means of the Metropolis algorithm, a Markov chain Monte Carlo method, well suited for calculating Ising model estimations.

Analytical expressions for the partition function and the corresponding expectation values for the energy and the absolute value of the mean magnetization will be derived for a 2×2 lattice Ising model. From these, expressions for the specific heat capacity, C_V , and the susceptibility, χ , will be derived as well. These results will serve as benchmark calculations when testing the implementation of the Metropolis algorithm for calculating Ising model estimations.

After verifying the implementation, the next subject of interest is how fast the system reaches equilibrium, or the most likely state. This will be studied by simulating the system for several temperatures and initial lattice orderings.

The behavior of the Metropolis algorithm will also be studied in terms of how the number of accepted states behaves as a function of temperature and the number of Monte Carlo cycles.

The next item in the study is the simulated probability distribution. This will be found by counting the relative frequency of different energy states for different temperatures. As a verification of the implementation, the variance of the distribution will be compared with the corresponding variance term in the expression for the specific heat capacity.

In the study of the phase transitions it is advantageous to parallelize the code, so this will be done. In order to verify that an optimal speedup is achieved, a time analysis will be performed on some selected runs.

Finally, the phase transitions are studied in a range of temperatures around the expected Curie temperature (after Lars Onsager) for different finite lattices. The study culminates in the extraction of the Curie temperature through finite scaling relations.

This project is structured by first presenting a theoretical overview of the Ising model, along with the physics behind, and the Metropolis algorithm in [Section 2](#). This is followed by a presentation on the approach to study the various Ising model estimations in [Section 3](#). Next, the results of the Ising model estimations generated by the implementation of the Metropolis algorithm are presented in [Section 4](#), before subsequently they and the approach are discussed and concluded upon in [Section 5](#) and [Section 6](#), respectively. Lastly, an outline of possible continuations of the model with respect to the implementation are presented in [Section 7](#).

2 Theory

2.1 A Short Review of Statistical Mechanics

In statistical mechanics, the canonical ensemble is a collection of various microstates that represent the possible states of a closed system¹ of fixed volume, in thermal equilibrium with a heat bath at a fixed temperature T [2, p. 193]. The probability, P , for the system to be in a state i with energy E_i , is given by the Boltzmann distribution [3, p. 422]

$$P(E_i; \beta) = \frac{1}{Z} e^{-\beta E_i}, \quad (2.1)$$

with $\beta = 1/k_B T$ being the inverse temperature where k_B is the Boltzmann constant, and Z being the partition function for the canonical ensemble defined as

$$Z = \sum_{j=1}^M e^{-\beta E_j}, \quad (2.2)$$

where the sum extends over all microstates M accessible to the system.

In general, the n -th moment of a probability distribution of the discrete random variable $X = x_i$, that is, the expected value of the n -th power of the random variable under consideration, is defined as

$$\langle X^n \rangle = \sum_i x_i^n P(X = x_i)$$

The zeroth moment, $\langle 1 \rangle$, is the normalization condition of the probability distribution. The first moment is the mean, denoted by μ_X , often simply called the expectation value since it represents the centroid value of the probability distribution. Furthermore, a moment about the mean, that is, the expected value of the n -th power of the deviation of the random variable from the mean, is called a central moment. The second central moment is the variance, denoted by σ_X^2 [3, p. 340-341].

Following, the mean energy of a canonical system can be evaluated through

$$\langle E \rangle = \mu_E = \sum_{i=1}^M E_i P(E_i; \beta) = \frac{1}{Z} \sum_{i=1}^M E_i e^{-\beta E_i}, \quad (2.3)$$

and the corresponding variance

$$\sigma_E^2 = \langle E^2 \rangle - \langle E \rangle^2 = \frac{1}{Z} \sum_{i=1}^M E_i^2 e^{-\beta E_i} - \left(\frac{1}{Z} \sum_{i=1}^M E_i e^{-\beta E_i} \right)^2 \quad (2.4)$$

The specific heat capacity, C_V , at a constant volume is obtained by dividing the latter quantity by $k_B T^2$ [3, p. 420]

$$C_V = \frac{1}{k_B T^2} (\langle E^2 \rangle - \langle E \rangle^2) \quad (2.5)$$

Similarly can the mean magnetization be evaluated through

$$\langle \mathcal{M} \rangle = \mu_{\mathcal{M}} = \sum_{i=1}^M \mathcal{M}_i P(E_i; \beta) = \frac{1}{Z} \sum_{i=1}^M \mathcal{M}_i e^{-\beta E_i}, \quad (2.6)$$

¹Energy can transfer between the system and the surroundings, but not mass.

and the corresponding variance

$$\sigma_{\mathcal{M}}^2 = \langle \mathcal{M}^2 \rangle - \langle \mathcal{M} \rangle^2 = \frac{1}{Z} \sum_{i=1}^M \mathcal{M}_i^2 e^{-\beta E_i} - \left(\frac{1}{Z} \sum_{i=1}^M \mathcal{M}_i e^{-\beta E_i} \right)^2 \quad (2.7)$$

The susceptibility, χ , at a constant volume is obtained by dividing the latter quantity by $k_B T$ [3, p. 420]

$$\chi = \frac{1}{k_B T} \left(\langle \mathcal{M}^2 \rangle - \langle \mathcal{M} \rangle^2 \right) \quad (2.8)$$

In the canonical ensemble, the thermodynamic potential is the Helmholtz free energy

$$F = -k_B T \ln Z, \quad (2.9)$$

which gives the relation $\ln Z = -F/k_B T = -F/\beta$.

2.2 The Ising Model

In statistical mechanics, the Ising model is a model of interacting magnetic dipole moments of atomic spins. The spins, denoted by S , are in either a spin up state, with numerical value $+1$ and depicted by \uparrow , or a spin down state, with numerical value -1 and depicted by \downarrow . The spins are usually arranged in a lattice, where each spin sets up a magnetic field related to the spin direction. This field will decay with the distance from spin S_i , so the interaction between spin S_i and S_j will therefore depend on the distance between the spins. As an approximation, the decay of the magnetic field will be assumed to happen rapidly in space, so that the interaction only is between the nearest neighbors [2, p. 211-212]. A lattice with a specific spin configuration corresponds to a microstate of the system. For N spin particles there are $M = 2^N$ possible microstates (or configurations). The energy of a specific configuration i for a system with N spin particles is then given by the Hamiltonian [3, p. 421]

$$H_i = - \sum_{\langle i, j \rangle}^N J_{ij} S_i S_j - \mathcal{B}_{\text{ext}} \sum_j^N S_j,$$

where $\langle i, j \rangle$ indicates that the sum is over the nearest neighbors only, \mathcal{B}_{ext} is an external magnetic field interacting with the magnetic moment set up by the spins, and J_{ij} is a coupling constant that includes the effect of the magnetic field set up by spin i , the decay of the field with distance, and the coupling between the field and spin S_j . In this project, the Ising model is examined without an external field interacting with the lattice, that is, $\mathcal{B}_{\text{ext}} = 0$. Furthermore, all of the nearest neighbors $\langle i, j \rangle$ is assumed to have the same interaction strength. Thus, the above equation simplifies to

$$E_i = -J \sum_{\langle i, j \rangle}^N S_i S_j \quad (2.10)$$

For $J > 0$ it is energetically favorable for neighboring spins to be aligned. Materials with $J > 0$ are ferromagnetic, and exhibit a long-range ordering phenomenon where a given magnetic moment, through interactions between nearest neighbors, can influence the alignment of spins that are separated from the given spin by a macroscopic distance. The appearance of an ordered spin state leads to a phenomenon called spontaneous magnetization, meaning that the lattice has a net magnetization even in the absence of an external magnetic field.

However, this property manifest itself only below a critical temperature, called the Curie temperature, T_C . For temperatures $T \geq T_C$ the ferromagnetic property disappears as a result of thermal agitation. It is also worth mentioning that the alignment of spins occur within a domain in the material, where different domains will themselves be randomly oriented so that a bulk sample of the material usually is not magnetized [3, p. 421-422][4].

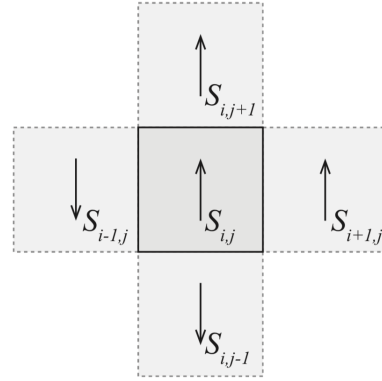
In the Ising model, the magnetization is given by [3, p. 423]

$$\mathcal{M}_i = \sum_{j=1}^N S_j, \quad (2.11)$$

where the sum is over all spins for a given configuration i .

Figure 2.1 illustrates the concept of “nearest neighbors” in a square lattice in two dimensions, where the spin $S_{i,j}$ sets up a magnetic field which interacts with the neighboring spins $S_{i-1,j}$, $S_{i+1,j}$, $S_{i,j-1}$, and $S_{i,j+1}$.

Figure 2.1: *Neighbors in the the two dimensional Ising model. The neighbors for a spin $S_{i,j}$ are $S_{i-1,j}$, $S_{i+1,j}$, $S_{i,j-1}$, and $S_{i,j+1}$. Figure retrieved from Fig. 7.8 in [2].*



For the remainder of this project, the magnetic system under consideration will have a ferromagnetic ordering, viz $J > 0$. Furthermore, the lattice under consideration will be two dimensional, that is, a square lattice with $L \times L$ spin sites, with L being the number of spins in one dimension.

2.3 Periodic Boundary Conditions

A physical crystal structure consists of a very large number of atoms. In order to model a crystal structure realistically, it usually requires a lattice essentially infinite in all directions. This implies that the behavior of the crystal near the boundaries of the lattice is effectively negligible for the crystal as a whole. It is infeasible to simulate a lattice even remotely approaching a very large number, due to limits of computation. Instead, the boundaries of a relatively small finite lattice must be handled in a manner that ensures a good correspondence with reality. With periodic boundary conditions, spins at the boundary will have its nearest neighbors at the opposite boundary. This ensures that the boundary of a finite lattice has no effect on the behavior of the crystal.

2.4 Analytical Expressions of the Ising Model

Here, the aim is to find analytical expressions for the partition function and the corresponding expectation values for the energy, E , and the absolute value of the mean magnetization, $|\mathcal{M}|$. From these, expressions for the specific heat capacity, C_V , and the susceptibility, χ , will be derived as well. For simplicity, the analytical expressions will be found for the 2×2 lattice Ising model with periodic boundary conditions. These results will serve as benchmark calculations when testing the implementation of the Metropolis algorithm for calculating Ising model estimations later on.

For a 2×2 lattice Ising model there are $M = 2^4 = 16$ possible microstates. [Table 2.1](#) group these configurations according to their total energy, given by [Equation \(2.10\)](#), and magnetization, given by [Equation \(2.11\)](#).

Table 2.1: Tallying of possible configurations and corresponding quantities for a 2×2 lattice Ising model with periodic boundary conditions. Here, N_\uparrow is the number of spin up states in the lattice configuration, Ω is the degeneracy of the microstate, E_i is the energy given by [Equation \(2.10\)](#), and \mathcal{M}_i is the magnetization given by [Equation \(2.11\)](#).

N_\uparrow	Ω	E_i	\mathcal{M}_i
4	1	$-8J$	4
3	4	0	2
2	4	0	0
2	2	$8J$	0
1	4	0	-2
0	1	$-8J$	-4

The partition function, introduced with [Equation \(2.2\)](#), for the 2×2 lattice Ising model with periodic boundary conditions is found by summing over all the possible microstates i , given by the table above;

$$Z = \sum_i e^{-\beta E_i} = 2e^{-\beta 8J} + 2e^{\beta 8J} + 12e^0 = 4 \cosh(\beta 8J) + 12 \quad (2.12)$$

As mentioned in [Section 2.1](#), the partition function can be used to derive several properties of a statistical ensemble. The mean energy can be derived from [Equation \(2.3\)](#), but it is here more practical to use the relation

$$\langle E \rangle = -\frac{\partial \ln Z}{\partial \beta} = -\frac{8J \sinh(\beta 8J)}{\cosh(\beta 8J) + 3} \quad (2.13)$$

For the corresponding variance, it is, however, more convenient to use [Equation \(2.4\)](#), where

$$\langle E^2 \rangle = \frac{1}{Z} \sum_i E_i^2 e^{-\beta E_i} = \frac{64J^2 \cosh(\beta 8J)}{\cosh(\beta 8J) + 3}$$

and

$$\langle E \rangle^2 = \left(\frac{1}{Z} \sum_i E_i e^{-\beta E_i} \right)^2 = \left(\frac{8J \sinh(\beta 8J)}{\cosh(\beta 8J) + 3} \right)^2$$

so that

$$\sigma_E^2 = \frac{64J^2 \cosh(\beta 8J)}{\cosh(\beta 8J) + 3} - \left(\frac{8J \sinh(\beta 8J)}{\cosh(\beta 8J) + 3} \right)^2 \quad (2.14)$$

The specific heat capacity, introduced with Equation (2.5), is thus given by

$$C_V = \frac{1}{k_B T^2} \left[\frac{64J^2 \cosh(\beta 8J)}{\cosh(\beta 8J) + 3} - \left(\frac{8J \sinh(\beta 8J)}{\cosh(\beta 8J) + 3} \right)^2 \right] \quad (2.15)$$

Similarly, the mean magnetization can be evaluated with Equation (2.6), but the mean magnetization for the 2×2 lattice Ising model with periodic boundary conditions evaluates to zero. However, the absolute value of the mean magnetization becomes

$$\langle |\mathcal{M}| \rangle = \frac{1}{Z} \sum_i |\mathcal{M}| e^{-\beta E_i} = \frac{2 + 4e^{\beta 8J}}{\cosh(\beta 8J) + 3} \quad (2.16)$$

Moving forward, the absolute value of the mean magnetization will simply be referred to as the mean magnetization. As for the energy, the corresponding variance of the magnetization is found by using Equation (2.7), where

$$\langle \mathcal{M}^2 \rangle = \frac{1}{Z} \sum_i \mathcal{M}_i^2 e^{-\beta E_i} = \frac{8e^{\beta 8J} + 8}{\cosh(\beta 8J) + 3}$$

and

$$\langle |\mathcal{M}| \rangle^2 = \left(\frac{1}{Z} \sum_i \mathcal{M}_i e^{-\beta E_i} \right)^2 = \left(\frac{2 + 4e^{\beta 8J}}{\cosh(\beta 8J) + 3} \right)^2,$$

so that

$$\sigma_{\mathcal{M}}^2 = \frac{8e^{\beta 8J} + 8}{\cosh(\beta 8J) + 3} - \left(\frac{2 + 4e^{\beta 8J}}{\cosh(\beta 8J) + 3} \right)^2 \quad (2.17)$$

The susceptibility, introduced with Equation (2.8), is thus given by

$$\chi = \frac{1}{k_B T} \left[\frac{8e^{\beta 8J} + 8}{\cosh(\beta 8J) + 3} - \left(\frac{2 + 4e^{\beta 8J}}{\cosh(\beta 8J) + 3} \right)^2 \right] \quad (2.18)$$

2.5 Second Order Phase Transitions in the Ising Model

A phase transition takes place when there is a clearly noticeable and sudden macroscopic change in a given medium as external parameters, such as temperature, are changed. The point where the phase transition occurs is called a critical point [3, p. 429]. A phase transition is normally characterized as either a first order or a second order transition. The former is discontinuous in the first derivative of the partition function or the free energy (see Equation (2.9)), whereas the latter is continuous in the first derivative but exhibit discontinuity in the second derivative of the partition function (or the free energy) [3, p. 430]. Both the specific heat capacity, C_V , and the magnetic susceptibility, χ , are given by a second derivative of the partition function (or the free energy), so both of these quantities diverge in a second order transition.

The two dimensional square lattice Ising model without an external magnetic field interacting with the lattice, undergoes a phase transition of second order. As discussed in [Section 2.2](#), this means that the Ising model exhibits a spontaneous magnetization, $\langle |\mathcal{M}| \rangle \neq 0$, below the Curie temperature T_C . Above T_C the magnetization is zero, $\langle |\mathcal{M}| \rangle = 0$. At T_C a so-called critical phenomena occurs; $\langle |\mathcal{M}| \rangle \rightarrow 0$ with an infinite slope. A critical phenomena is, in general, characterized by one or more thermodynamic variables which vanishes above a critical point in the thermodynamic limit, that is, with an infinitely large lattice. Such a variable is usually called the order parameter, in this case the mean magnetization [[3](#), p. 430-431].

In this project, the aim is to extract the Curie temperature T_C . An important quantity in studies of phase transitions is the correlation length ξ , which is related to the spin-correlation (which again defines the magnetic susceptibility χ). For $T \gg T_C$, ξ is expected to be of the order of the lattice spacing. As $T \rightarrow T_C$, the correlation length increases as a consequence of stronger spin correlation. The discontinuous behavior of ξ near T_C is [[3](#), pp. 430-431]

$$\xi(T) \sim |T_C - T|^{-\nu} \quad (2.19)$$

In the actual calculations of the square lattice Ising model, the lattice under consideration is limited to always be of a finite dimension (see [Section 2.3](#)). ξ will then be proportional to the size of the lattice at the critical point, that is

$$\xi(T) \propto L \sim |T_C - T|^{-\nu}$$

Through finite scaling relations, the behavior at finite lattices can be related with the results for an infinitely large lattice, and the Curie temperature then scales as [[3](#), p. 431-431]

$$T_C(L) - T_C(L = \infty) = aL^{-1/\nu}, \quad (2.20)$$

where a is a constant and ν is defined by [Equation \(2.19\)](#). Since the lattice will be of a finite dimension, both C_V and χ will not exhibit diverging behavior. Instead, there will be a noticeable maximum in both quantities near T_C . The sharpness of these peaks will increase as L increases.

The exact result gives that $\nu = 1$. Thus [Equation \(2.20\)](#) can be rewritten as the linear relation

$$T_C(L) = aL^{-1} + T_C(L = \infty) \quad (2.21)$$

The exact result for the Curie temperature, given by Onsager [[1](#)], is

$$k_B T_C / J = \frac{2}{\ln(1 + \sqrt{2})} \approx 2.269 \quad (2.22)$$

2.6 The Metropolis Algorithm

The Metropolis algorithm is a Markov chain Monte Carlo (MCMC) method for sampling the expectation of a statistic in a model for which direct sampling is difficult. The principle of a Monte Carlo simulation is to let the computer perform N experiments, or measurements, where the outcome is random within some probability distribution. One such experiment constitutes a Monte Carlo cycle, so N experiments, in this sense, correspond to N Monte

Carlo cycles. A statistic occurring M times thus have the probability M/N . In simulating the Ising model, the main idea is to generate a sequence of consecutive states by changing the microstates at random by flipping spins. A naive Monte Carlo method would be to sample completely at random. However, the probability of a state i is given by the Boltzmann distribution (Equation (2.1)), so the microstates are not equally probable. This means that each of the microstates in the sequence do not weigh equally when the average of a statistic is calculated. Ideally, the choice of random states should be guided by weighing the importance of a microstate i with energy E_i according to the probability. This is called importance sampling, and the idea is to generate a sequence of probable microstates which still conserves a sufficient random sample of the microstates. Such a sequence is called a Markov chain [2, p. 255-256][3, p. 381-382].

The Metropolis algorithm is thus an importance sampling method, which generates a sequence of states. The algorithm chooses selection probabilities $P(i, j)$ which represent the probability that state j is selected as the consecutive state to i . Whether the state j is retained or not is determined according to an acceptance rule. [3, p. 400-401]

In a calculation of the square lattice Ising, the number of microstates is given by $M = 2^N$ with $N = L \times L$ number of spins for a lattice of length L . The canonical partition function, given by Equation (2.2), is therefore troublesome to compute for even moderately large systems, since all states are needed. Luckily, the principle of detailed balance gives [3, p. 403]

$$\frac{P(i, j)}{P(j, i)} = \frac{P(j)}{P(i)} = \frac{(e^{-\beta E_j})/Z}{(e^{-\beta E_i})/Z} = e^{-\beta \Delta E}, \quad (2.23)$$

which is called the acceptance amplitude where $\Delta E = E_j - E_i$. In the Metropolis algorithm, Equation (2.23) serves as the acceptance rule. In addition, if the energy of a new configuration is lower than the previous, the change must also be accepted.

The Metropolis algorithm conserves two important properties of the system:

1. The tendency to minimize energy, that is, reach the most likely state (equilibrium).
2. Ergodicity, that is, the system must be able to assume all possible states given enough time.

The 2nd property listed above means that the energy must be allowed to fluctuate to higher energies.

The steps of the Metropolis algorithm itself are presented in the next section.

3 Method

3.1 Implementing the Metropolis Algorithm

Note: All quantities in this project are manipulated in normalized units, that is, temperature is normalized, the Boltzmann constant $k_B \sim 1$, and the coupling strength is taken as $J = 1$.

The Metropolis algorithm will be implemented with the procedure outlined below [2, p. 258] [3, p. 435].

1. Establish an initial microstate with energy E_i and either a random or an ordered spin configuration.
2. Make a random change in the microstate, that is, a trial state, by flipping a spin at a random site. Compute the energy E_j of the trial state.
3. Calculate $\Delta E = E_j - E_i$. The number of values ΔE is limited to five for the square lattice Ising model. See the discussion below.
4. If $\Delta E \leq 0$, accept the new configuration since the energy is lowered and the system is hopefully moving towards equilibrium. Go to step 7.
5. If $\Delta E > 0$, generate a random number, r , between 0 and 1. Go to step 6.
6. If $r \leq e^{-\beta\Delta E}$, accept the new configuration, else keep the old configuration.
7. Update the expectation values.
8. Repeat step 2-7 until a sufficiently good representation of states is obtained.
9. A sweep over the lattice is performed by summing over all the spins. A sweep constitutes a Monte Carlo cycle, where one such cycle is a measurement of the system. At the end of all cycles, the expectation values are divided by the total number of cycles. By also dividing by the number of spins, the results will be per spin.

For the square lattice Ising model there are only five possible values of ΔE , namely $\Delta E = 8J, 4J, 0, -4J, -8J$. This means that $e^{-\beta\Delta E}$ can be precalculated and stored in i.e. an array outside the Monte Carlo loop, thus avoiding evaluating the exponential at each Monte Carlo sampling.

The periodic boundary conditions discussed in [Section 2.3](#) will also be included in the implementation of the Ising model.

[Figure 3.1](#) depicts a flowchart of the algorithm steps outlined above.

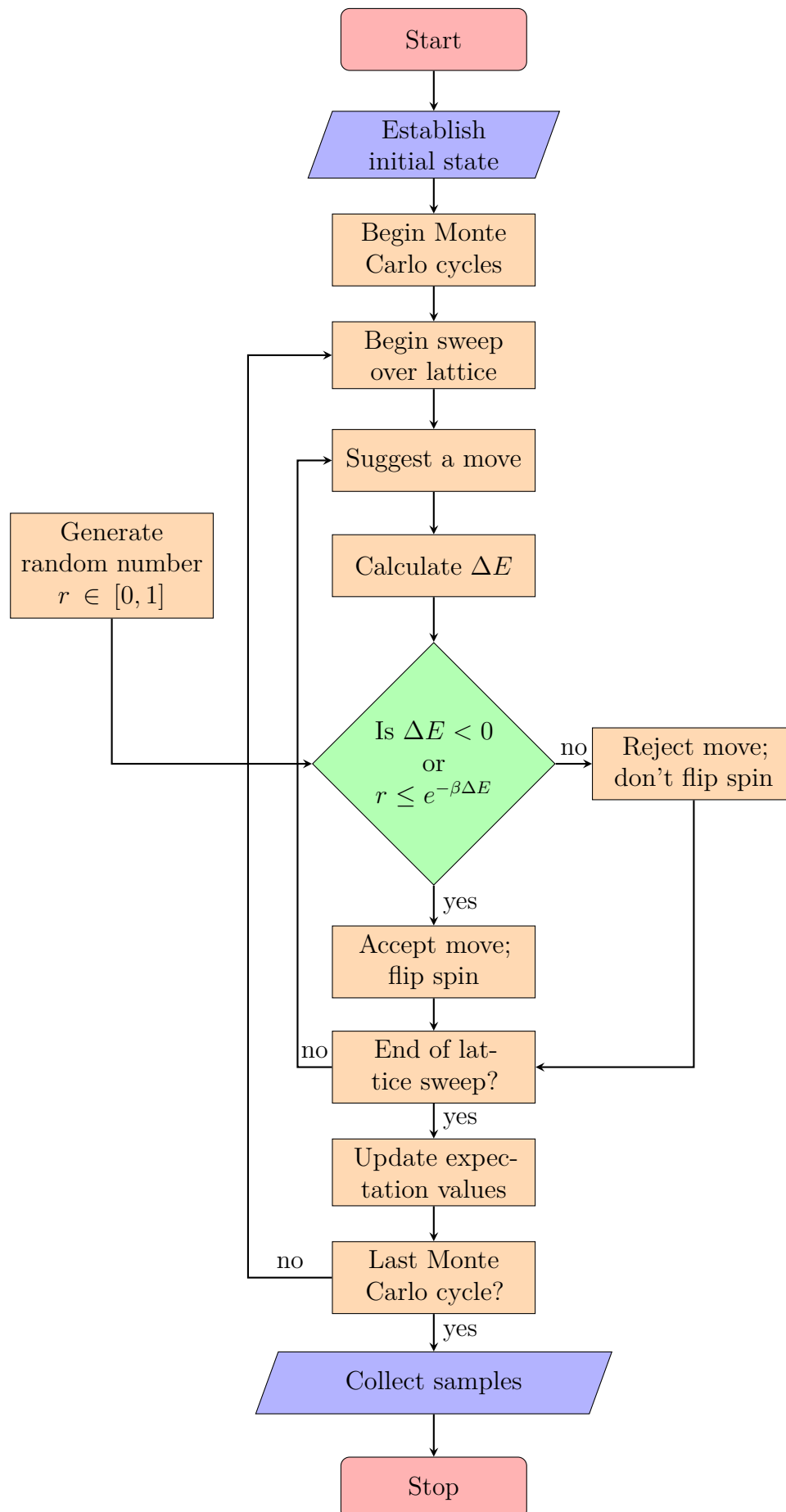


Figure 3.1: Flowchart of the Metropolis algorithm based on the steps outlined in the body text. Modified from Fig. 12.7 in [3].

3.2 Verifying the Implementation

As mentioned in [Section 2.4](#), the analytic expressions for the 2×2 lattice Ising model with periodic boundary conditions will here be used to verify the implementation of the Metropolis algorithm. The estimated values for the quantities mean energy $\langle E \rangle$, (absolute value of) mean magnetization $\langle |\mathcal{M}| \rangle$, specific heat capacity C_V , and susceptibility χ generated with $N = 10^3, 10^4, 10^5, 10^6, 10^7$ Monte Carlo cycles, will be compared to their analytic counterparts given by [Equation \(2.13\)](#), [Equation \(2.16\)](#), [Equation \(2.15\)](#), and [Equation \(2.18\)](#), respectively. Both the analytical and numerical results will be calculated per spin, L^2 . The results will be presented in a table.

Next, a similar analysis will be performed, but with all quantities as a function of temperature in a range $T \in [1, 3]$ with step $\Delta T = 0.01$. The results will be presented in three main figures, one for each number of Monte Carlo cycles, $N = 10^3, 10^4, 10^6$.

3.3 Equilibrium for Ordered and Disordered Initial State

In order to investigate the time the system needs to reach equilibrium, the evolution of the total energy and magnetization per spin will be plotted as a function of the number of Monte Carlo cycles N for a 20×20 lattice. This will be done for both a disordered (random) and an ordered initial state, with both temperatures $T = 1$ and $T = 2.4$. Each quantity will be plotted in separate main figures, where one main figure shows the evolution for both the initial states for a given temperature.

The rationale behind looking at the total energy and magnetization instead of the expectation values, is that the latter may still be skewed long after the system has equilibrated.

3.4 Number of Accepted States

Here, the number of accepted states, that is, states that pass the test in step 4 or 6 mentioned in [Section 3.1](#), will be counted. The evolution of the number of accepted states as a function of the number of Monte Carlo cycles will be presented in a figure. A figure of the number of accepted states per sweep as a function of temperature will also be presented. The lattice will maintain the size of 20×20 .

3.5 Probability Distribution

The next subject of the study is to find a probability distribution, $P(E_i)$, for the previous system with $L = 20$ and the same temperatures $T = 1$ and $T = 2.4$. This will be done by simulating the evolution of the total energy of each cycle at a given temperature, and extract the relative frequency of each unique energy state. The result will be presented in a figure.

As a verification of the implementation, the variance, σ_E^2 , of the distribution will be compared with the corresponding variance term in the expression for the specific heat capacity, given by [Equation \(2.5\)](#).

3.6 Studies of Phase Transitions

Next, the behavior of the square lattice Ising model in a temperature domain around the expected Curie temperature will be studied. Computations of the mean energy $\langle E \rangle$, mean magnetization $\langle |\mathcal{M}| \rangle$, heat capacity C_V , and magnetic susceptibility χ as functions of temperature in an interval $T \in [2.2, 2.4]$ with step $\Delta T = 0.05$, $N = 10^6$ Monte Carlo cycles, and 1000 precycles will be performed. In order to capture the interesting properties, the computation will be done with several lattice sizes, specifically $L = 40, 60, 100, 160$. The results for each quantity will be presented in separate figures.

The code used here will be parallelized.

3.7 Parallelization Speedup

In order to ascertain if the parallelized code gives an optimal speedup, a timing analysis of the CPU time will be performed on some selected runs with and without parallelization (MPI). In the first comparison, the CPU times for $N = 10^5$ Monte Carlo cycles and zero precycles will be measured. In the second comparison, the CPU times for $N = 10^5$ Monte Carlo cycles and 1000 precycles will be measured. The results from each comparison will be presented in separate tables, with the ratio of the times included.

The parallelization will be done on eight threads, whereas the run without parallelization on one thread. Furthermore, the parallelization will be implemented fairly straightforward by running a unique Metropolis simulation on each thread, seeded differently, and collecting all sampled values at the end.

3.8 Extracting the Curie Temperature

In the grand finale of this study, the Curie temperature T_C in the thermodynamic limit (infinitely large lattice) will be estimated based on the results with finite lattices outlined in [Section 3.6](#), specifically the result for the magnetic susceptibility χ (though the result for the specific heat capacity could also be used, in principle). Through the finite size scaling relation introduced in [Section 2.5](#), the Curie temperature in the thermodynamic limit is related to the finite lattice case with the linear relation given by [Equation \(2.21\)](#), restated below:

$$T_C(L) = aL^{-1} + T_C(L = \infty)$$

This means that by extracting the temperatures at the maximum values of χ for the different lattices in the computations of χ , these values can be linearly fitted as a function of $1/L$. The estimated $T_C(L = \infty)$ can then be read off from the constant factor.

4 Results

4.1 Implementing the Metropolis Algorithm

The programs containing the implementations of the Metropolis algorithm and the Ising model, as well as accompanying programs that produces all the results presented in this project, can be found at the GitHub repository

<https://github.com/nicolossus/FYS3150/tree/master/Project4>

4.2 Verifying the Implementation

Table 4.1 tabulates the numerical calculations for the expectation values, as well as the specific heat capacity and the susceptibility, all per spin, for the 2×2 lattice Ising model with N Monte Carlo cycles and temperature $T = 2$. The analytical solutions are also listed in the table.

Table 4.1: Table of mean energy, $\langle E \rangle$, (absolute value of) mean magnetization, $\langle |\mathcal{M}| \rangle$, specific heat capacity, C_V , and susceptibility, χ , estimations, all per spin L^2 , for different numbers of Monte Carlo cycles N with temperature $T = 2$. Analytical values are also listed for comparison.

N	$\langle E \rangle / L^2$	$\langle \mathcal{M} \rangle / L^2$	C_V / L^2	χ / L^2
10^3	-1.778	0.928	0.40272	0.095632
10^4	-1.791	0.93095	0.37672	0.093414
10^5	-1.80125	0.9341	0.35812	0.090544
10^6	-1.80119	0.93393	0.36073	0.090415
10^7	-1.80072	0.93366	0.36129	0.090893
Analytical	-1.8008	0.93371	0.36110	0.090798

Figure 4.1, Figure 4.2, and Figure 4.3 shows the quantities $\langle E \rangle$, $\langle |\mathcal{M}| \rangle$, C_V , and χ as functions of temperature, all per spin, L^2 . The plots have been generated by using $N = 10^3$, 10^4 , and 10^6 Monte Carlo cycles, respectively, with the temperature step $\Delta T = 0.01$. The analytical results are also included.

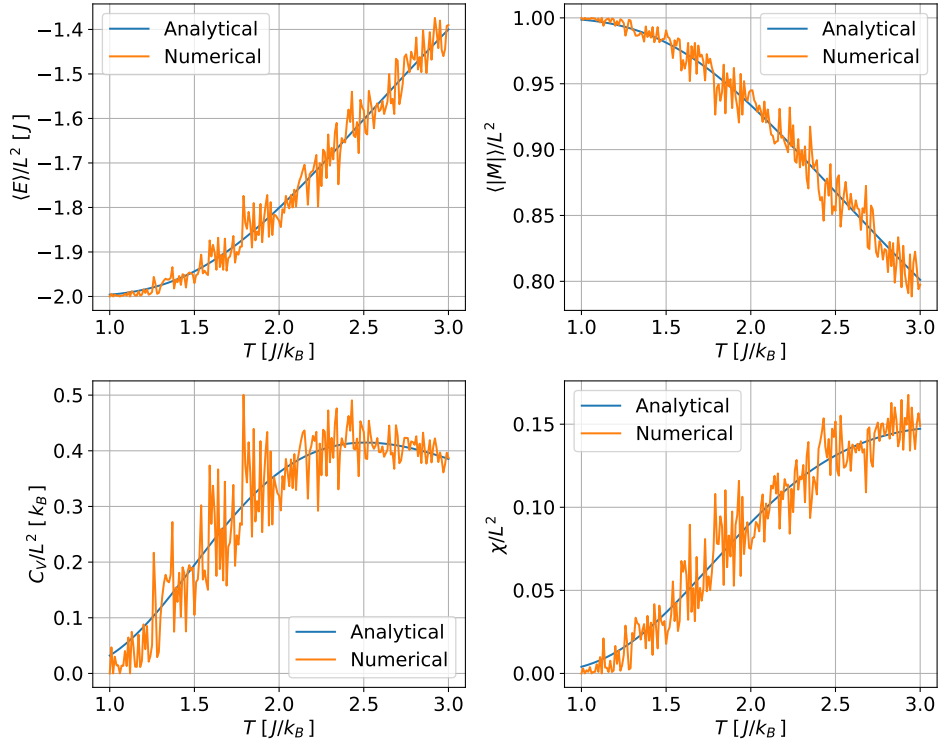


Figure 4.1: Comparison of exact and simulated results of $\langle E(T) \rangle / L^2$, $\langle |\mathcal{M}(T)| \rangle / L^2$, $C_V(T) / L^2$, and $\chi(T) / L^2$ for the $\times 2$ lattice Ising model. The results have been generated with $N = 10^3$ Monte Carlo cycles and temperature step $\Delta T = 0.01$.

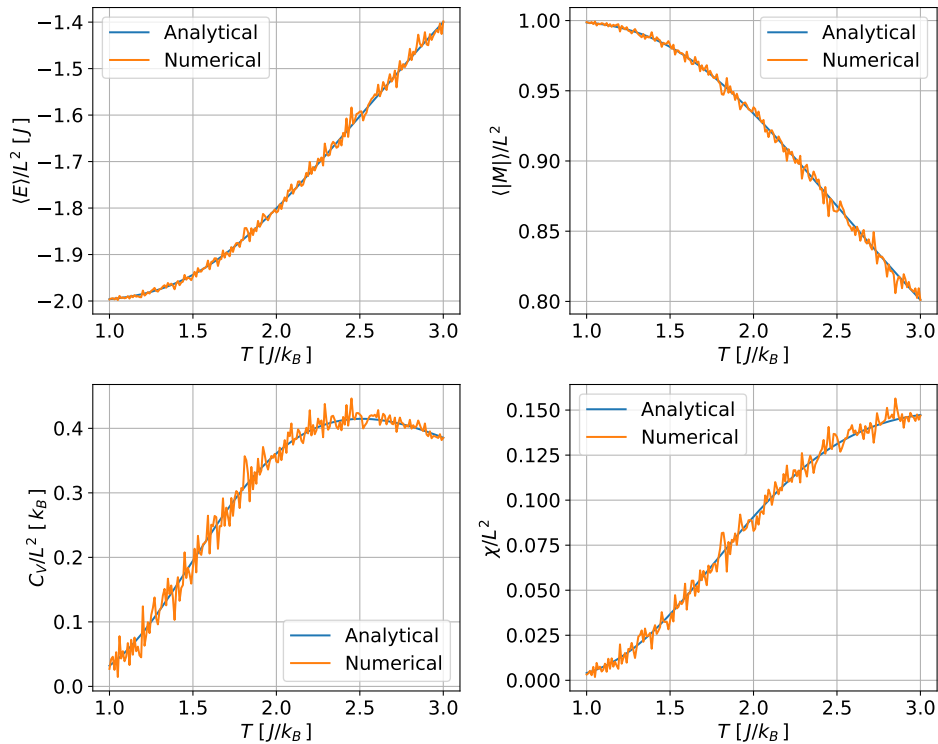


Figure 4.2: Comparison of exact and simulated results of $\langle E(T) \rangle / L^2$, $\langle |\mathcal{M}(T)| \rangle / L^2$, $C_V(T) / L^2$, and $\chi(T) / L^2$ for the $\times 2$ lattice Ising model. The results have been generated with $N = 10^4$ Monte Carlo cycles and temperature step $\Delta T = 0.01$.

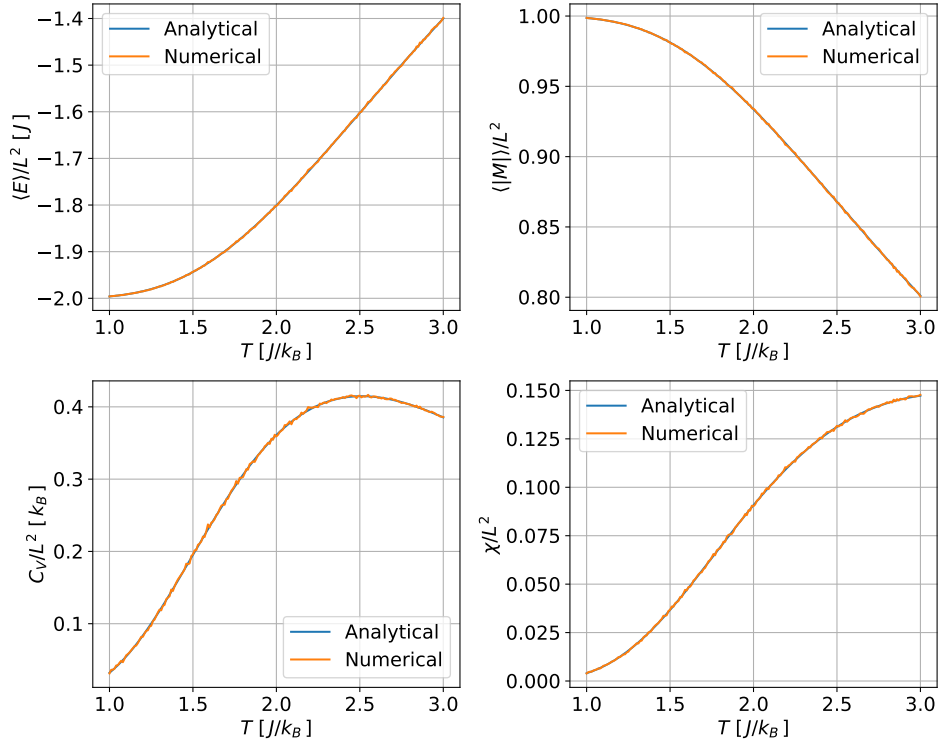


Figure 4.3: Comparison of exact and simulated results of $\langle E(T) \rangle / L^2$, $\langle |\mathcal{M}(T)| \rangle / L^2$, $C_V(T) / L^2$, and $\chi(T) / L^2$ for the $\times 2$ lattice Ising model. The results have been generated with $N = 10^6$ Monte Carlo cycles and temperature step $\Delta T = 0.01$.

4.3 Equilibrium for Ordered and Disordered Initial State

Figure 4.4 shows the evolution of the total energy as a function of the number of Monte Carlo cycles for a 20×20 lattice with both a disordered (random) and ordered initial state. The temperature is set to $T = 1$ and the number of Monte Carlo cycles is 2000.

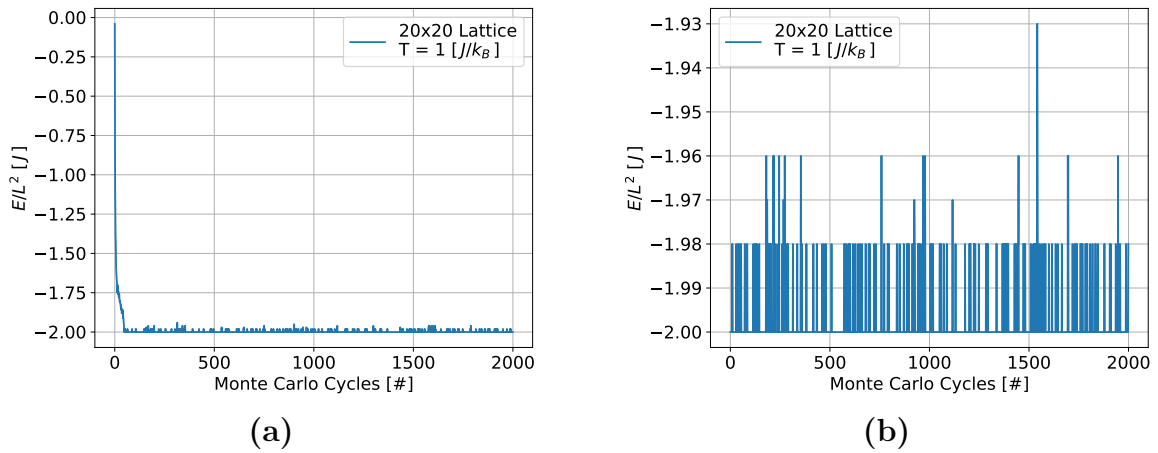


Figure 4.4: Evolution of the total energy as a function of the number of Monte Carlo cycles for a 20×20 lattice with $N = 2000$ Monte Carlo cycles and temperature $T = 1$. The initial state of the lattice is: **(a)** disordered **(b)** ordered.

Figure 4.5 shows the evolution of the total magnetization as a function of the number of Monte Carlo cycles for a 20×20 lattice with both a disordered (random) and ordered initial state. The temperature is set to $T = 1$ and the number of Monte Carlo cycles is 2000.

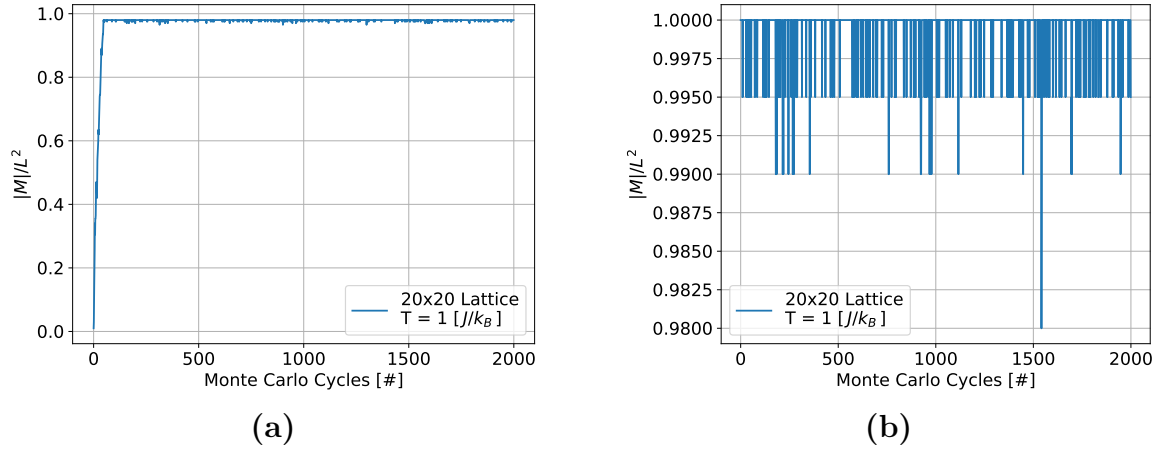


Figure 4.5: Evolution of the total magnetization as a function of the number of Monte Carlo cycles for a 20×20 lattice with $N = 2000$ Monte Carlo cycles and temperature $T = 1$. The initial state of the lattice is: **(a)** disordered **(b)** ordered.

Figure 4.6 shows the evolution of the total energy as a function of the number of Monte Carlo cycles for a 20×20 lattice with both a disordered (random) and ordered initial state. The temperature is set to $T = 2.4$ and the number of Monte Carlo cycles is 2000.

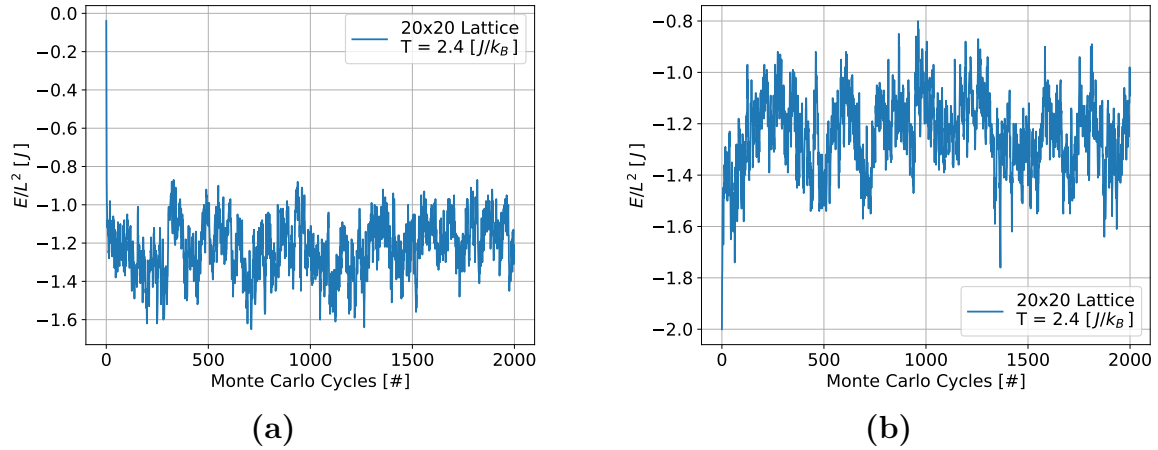


Figure 4.6: Evolution of the total energy as a function of the number of Monte Carlo cycles for a 20×20 lattice with $N = 2000$ Monte Carlo cycles and temperature $T = 2.4$. The initial state of the lattice is: **(a)** disordered **(b)** ordered.

Figure 4.7 shows the evolution of the total magnetization as a function of the number of Monte Carlo cycles for a 20×20 lattice with both a disordered (random) and ordered initial state. The temperature is set to $T = 1$ and the number of Monte Carlo cycles is 2000.

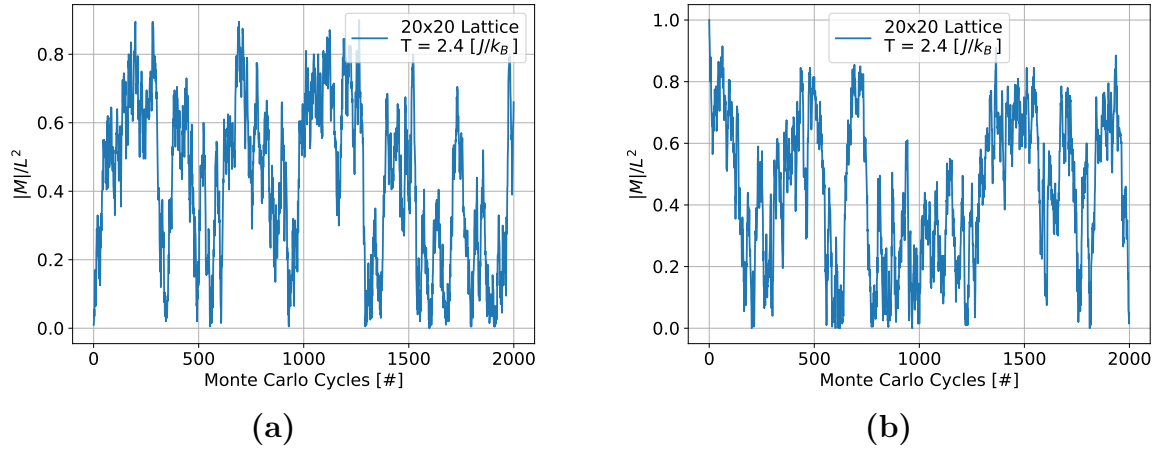


Figure 4.7: Evolution of the total magnetization as a function of the number of Monte Carlo cycles for a 20×20 lattice with $N = 2000$ Monte Carlo cycles and temperature $T = 2.4$. The initial state of the lattice is: (a) disordered (b) ordered.

4.4 Number of Accepted States

Figure 4.8 shows the number of accepted states as a function of the number of Monte Carlo cycles. The plot was generated by simulating a 20×20 lattice with temperature $T = 2$.

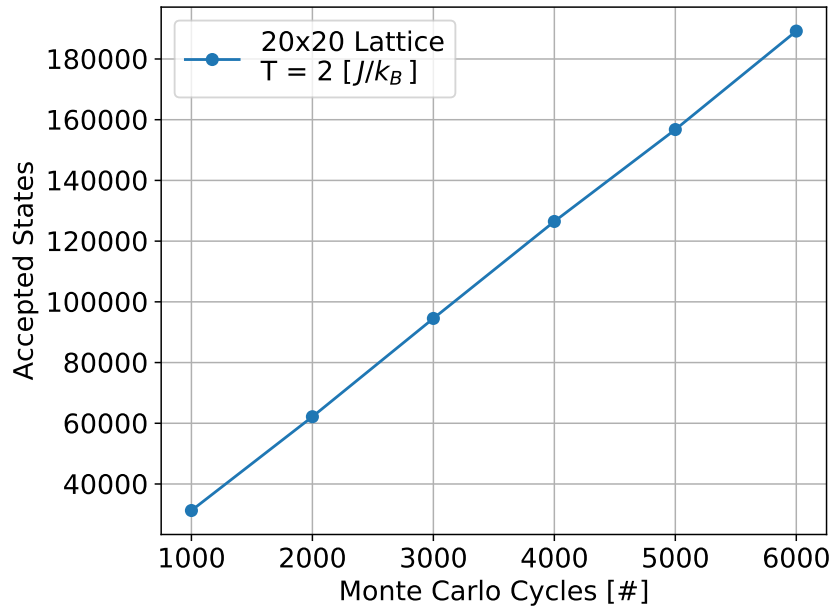


Figure 4.8: The number of accepted states as a function of the number of Monte Carlo cycles generated for a 20×20 lattice with a temperature $T = 2$.

Figure 4.9 shows the number of accepted states per sweep as a function of temperature. The plot was generated by simulating a 20×20 lattice with $N = 10^4$ Monte Carlo cycles.

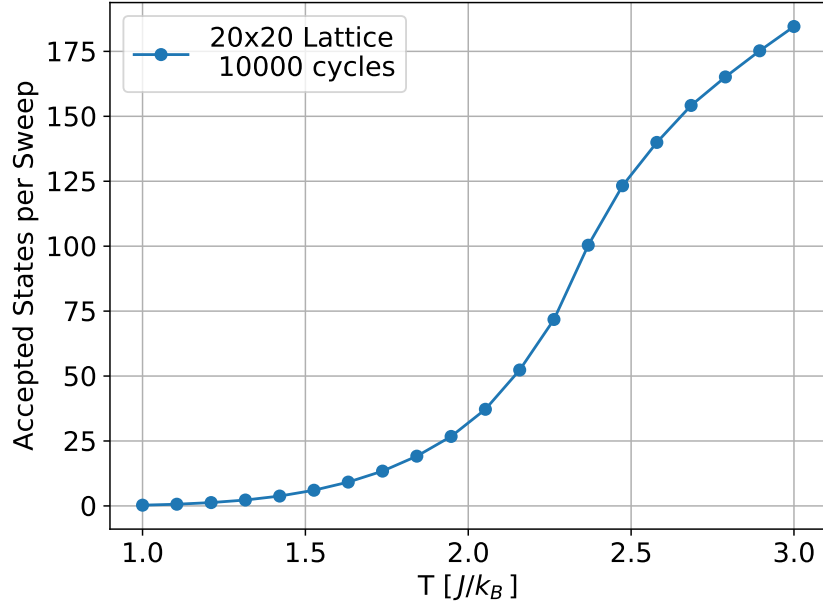


Figure 4.9: The number of accepted states per sweep as a function of the temperature. The plot was generated for a 20×20 lattice with $N = 10^4$ Monte Carlo cycles.

4.5 Probability Distribution

Figure 4.10 shows the relative frequency of unique energy states for a 20×20 lattice with both temperature $T = 1$ and $T = 2.4$. The plot was generated with $N = 10^{104}$ Monte Carlo cycles and 1000 precycles.

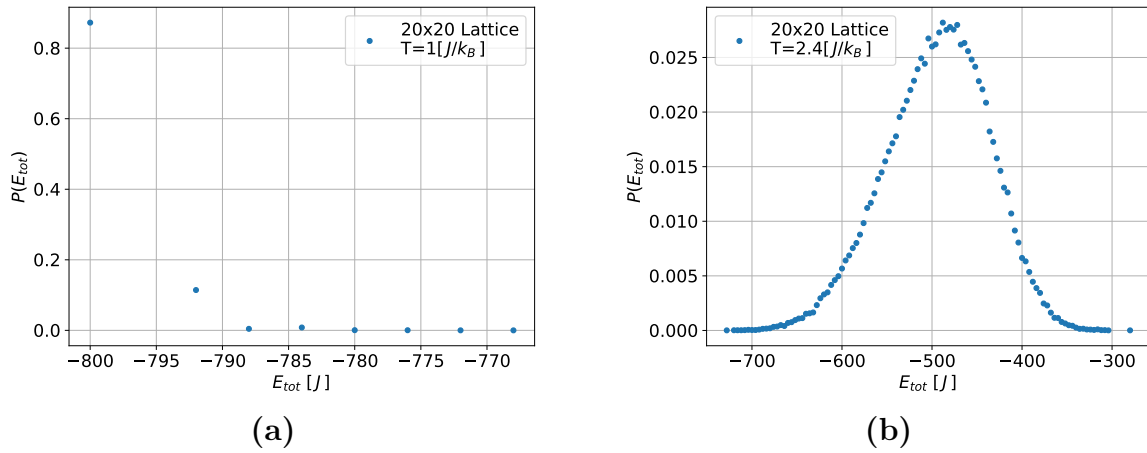


Figure 4.10: Relative frequency of unique energy levels for a 20×20 lattice generated with $N = 10^4$ Monte Carlo cycles and 1000 precycles. The temperature in: (a) $T = 1$ (b) $T = 2.4$.

The variance of the energy, σ_E^2 , calculated from the simulated heat capacity by reordering Equation (2.5), is

$$\sigma_E^2 = 9.216 \quad \text{for } T = 1$$

and

$$\sigma_E^2 = 3258 \quad \text{for } T = 2.4$$

4.6 Studies of Phase Transitions

Figure 4.11 shows the mean energy as a function of temperature in an interval around to the expected Curie temperature T_C . The chosen interval of the temperature is $T \in [2.2, 2.4]$ with a step size of $\Delta T = 0.05$, and the simulation is done for for several lattice sizes, specifically $L = 40, 60, 100, 160$, with $N = 10^6$ Monte Carlo cycles.

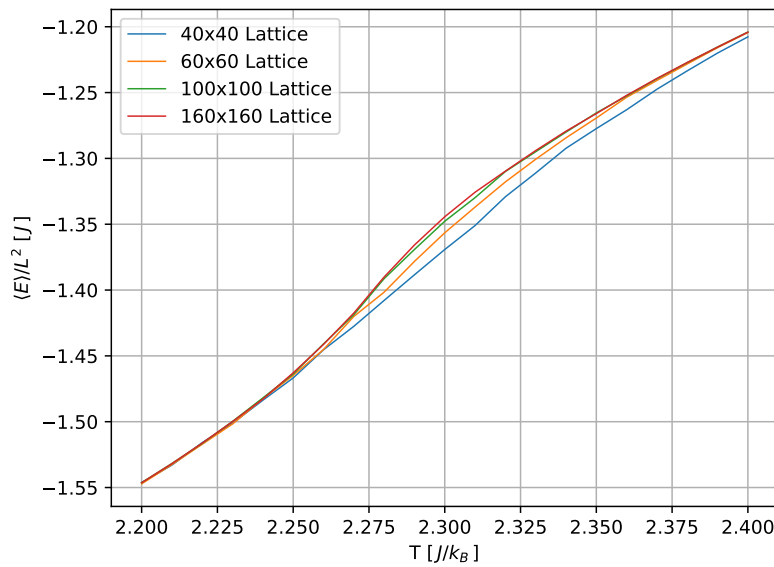


Figure 4.11: Mean energy as a function of temperature in an interval, $T \in [2.2, 2.4]$, around the expected Curie temperature. The simulation is done for various lattice sizes, specifically $L = 40, 60, 100, 160$, with a step size $\Delta T = 0.05$ and $N = 10^6$ Monte Carlo cycles.

Figure 4.12 shows the mean magnetization as a function of temperature in an interval around to the expected Curie temperature T_C . The chosen interval of the temperature is $T \in [2.2, 2.4]$ with a step size of $\Delta T = 0.05$, and the simulation is done for for several lattice sizes, specifically $L = 40, 60, 100, 160$, with $N = 10^6$ Monte Carlo cycles.

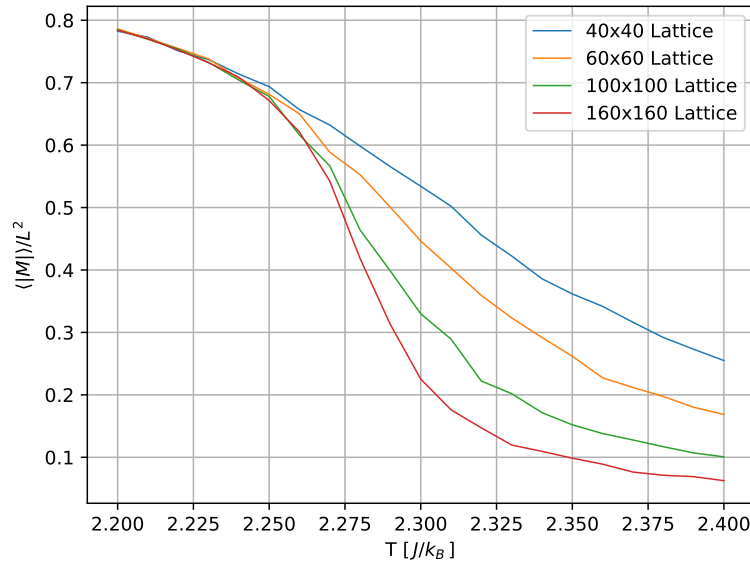


Figure 4.12: Mean magnetization as a function of temperature in an interval, $T \in [2.2, 2.4]$, around the expected Curie temperature. The simulation is done for various lattice sizes, specifically $L = 40, 60, 100, 160$, with a step size $\Delta T = 0.05$ and $N = 10^6$ Monte Carlo cycles.

Figure 4.13 shows the specific heat capacity as a function of temperature in an interval around to the expected Curie temperature T_C . The chosen interval of the temperature is $T \in [2.2, 2.4]$ with a step size of $\Delta T = 0.05$, and the simulation is done for for several lattice sizes, specifically $L = 40, 60, 100, 160$, with $N = 10^6$ Monte Carlo cycles.

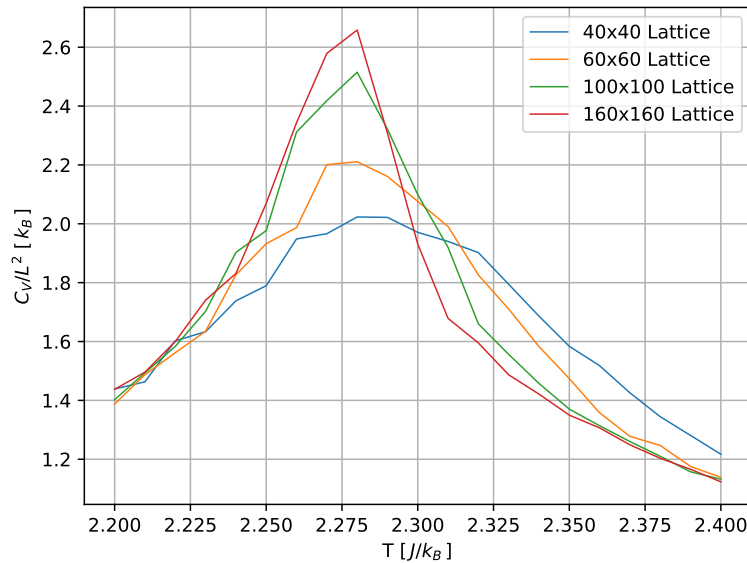


Figure 4.13: Specific heat capacity as a function of temperature in an interval, $T \in [2.2, 2.4]$, around the expected Curie temperature. The simulation is done for various lattice sizes, specifically $L = 40, 60, 100, 160$, with a step size $\Delta T = 0.05$ and $N = 10^6$ Monte Carlo cycles.

Figure 4.14 shows the susceptibility as a function of temperature in an interval around to the expected Curie temperature T_C . The chosen interval of the temperature is $T \in [2.2, 2.4]$ with a step size of $\Delta T = 0.05$, and the simulation is done for several lattice sizes, specifically $L = 40, 60, 100, 160$, with $N = 10^6$ Monte Carlo cycles.

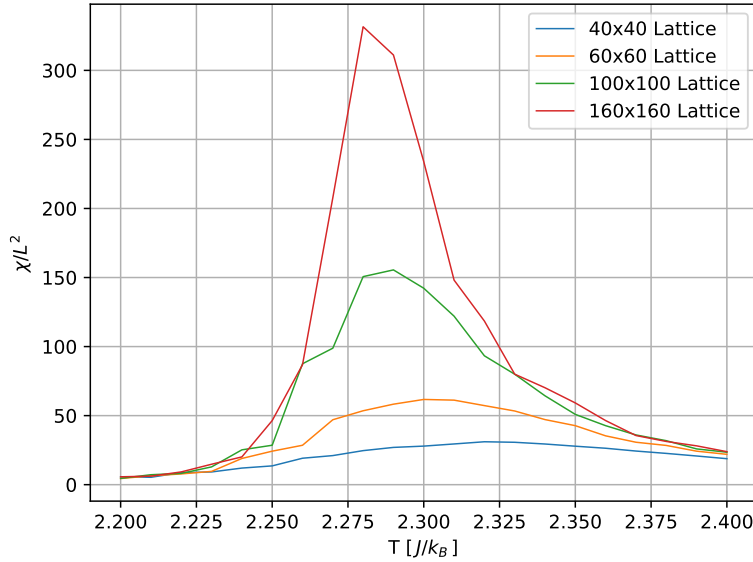


Figure 4.14: susceptibility as a function of temperature in an interval, $T \in [2.2, 2.4]$, around the expected Curie temperature. The simulation is done for various lattice sizes, specifically $L = 40, 60, 100, 160$, with a step size $\Delta T = 0.05$ and $N = 10^6$ Monte Carlo cycles.

4.7 Parallelization Speedup

In Table 4.2 and Table 4.3 are comparisons of the CPU times with and without parallelization. The parallelization is done on eight threads, whereas the run without parallelization is done on one thread. The tables also tabulates the ratio between the two times, which will show the relative speed up. The times in Table 4.2 are found with zero precycles, and the times in Table 4.3 are found with 1000 precycles.

Table 4.2: Comparison of CPU times with and without parallelization (MPI) for $N = 10^5$ Monte Carlo cycles and zero precycles. The ratio of times is also calculated, showing the relative speed up.

N	With MPI [s]	Without MPI [s]	Ratio
10^5	0.48	2.65	5.56

Table 4.3: Comparison of CPU times with and without parallelization (MPI) for $N = 10^5$ Monte Carlo cycles and 1000 precycles. The ratio of times is also calculated, showing the relative speed up.

N	With MPI[s]	Without MPI[s]	Ratio
10^5	0.56	2.79	4.98

4.8 Extracting the Curie Temperature

Figure 4.15 shows the Curie temperature as a function of $1/L$. The plot is generated by extracting the temperatures at the maximum values of the susceptibility for the different lattices in Figure 4.14 and linearly fitting the values in order to find the best estimate.

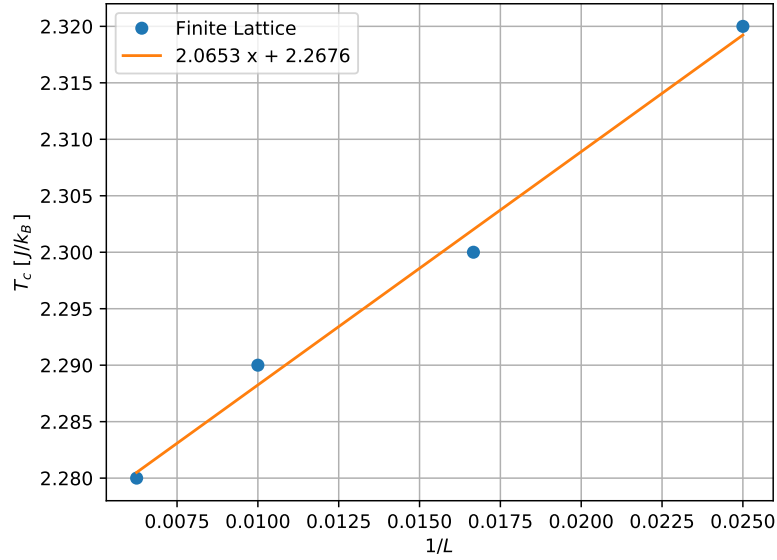


Figure 4.15: The Curie temperature T_C as a function of $1/L$. The data points corresponds to maximum temperature values from the simulations of the susceptibility χ with finite lattices, specifically $L = 40, 60, 100, 160$. The data points have been linearly fitted in order to find the best estimate for T_C . The Curie temperature is read of from the linear function as the constant term, stated in the plot legend.

Reading of the fitted linear constant term in the plot legend, gives that the best estimate of the extracted Curie temperature is

$$k_B T_C / J = 2.2676 \approx 2.268$$

5 Discussion

5.1 Implementing the Metropolis Algorithm

When implementing the Metropolis algorithm, the code (see [GitHub](#)) was written with object oriented code. The `Ising` class initializes the Ising model in two dimensions and calculates all the thermodynamic quantities. The `Metropolis` class contains a fairly general recipe for the iterative steps in the Metropolis algorithm, and is instructed to make an instance of the `Ising` class. The model in the `Ising` class can be extended to include more features, such as an external magnetic field, with reasonably ease.

Some disadvantages of the Metropolis algorithm in general, is that it typically only makes small changes to the states in each step. The states in the sequence will therefore be correlated. In addition, if the sequence is initialized with an unlikely state, it may take some time until the system reaches the most likely state (equilibrium).

5.2 Verifying the Implementation

[Table 4.1](#) shows that the numerical precision increases with the number of Monte Carlo cycles. Comparing the analytical results for the 2×2 lattice at $T = 2$ with the numerical obtained with $N = 10^7$ Monte Carlo cycles yields a relative error of order 10^{-5} , 10^{-5} , 10^{-4} and 10^{-3} for the mean energy, absolute value of mean magnetization, specific heat capacity, and magnetic susceptibility, respectively. The numerical results are thus fairly precise, given that the number of cycles is sufficient.

Initially the number of Monte Carlo cycles were chosen to be $N = 10^7$ for the simulations in this project. However, this number had a dramatically prolonged simulation time compared to $N = 10^6$. The latter number of Monte Carlo cycles was therefore settled on being acceptable for most of the following simulations when weighing performance and accuracy.

[Figure 4.1](#), [Figure 4.2](#), and [Figure 4.3](#) confirms that the trend of convergence holds for a more general range of temperatures. For lower N the fluctuation is substantial, but the deviation decreases as N increases.

All results considered, does the benchmark bolster confidence that the model also will remain accurate for larger lattices with a suitable number of Monte Carlo cycles.

5.3 Equilibrium for Ordered and Disordered Initial State

[Figure 4.4\(a\)](#) shows that the energy evolution of the lattice initialized with a disordered state at $T = 1$ begins at nearly zero. This is expected since the spin alignments are random and their energy contributions will tend to cancel each other. From the 1st cycle to $\sim 50^{\text{th}}$ cycle there is a steep drop towards the lowest energy available. Here, the energy reach the most likely state (equilibrium), but still fluctuates to higher energies (albeit, not much higher energies).

[Figure 4.4\(b\)](#) shows that the energy evolution of the lattice initialized with an ordered state at $T = 1$ appears to already be at equilibrium. This is expected since all the spins are aligned

so that the initial state has the lowest energy. The energy seems to fluctuate in the same manner as for the disordered initial state (after reaching equilibrium).

Figure 4.5(a) and Figure 4.5(b) shows the same trend as the total energy for the total magnetization at $T = 1$.

Figure 4.6(a) shows that the energy evolution of the lattice initialized with a disordered state at $T = 2.4$ again begins at nearly zero. However, here the system reaches equilibrium in far fewer cycles than the previous case. The number of cycles it needs to reach the most likely state is hard to extract from the figure, but it is most certainly a small number. With an increase in temperature, the most likely state is a bit higher than the lowest energy available. The fluctuations here are more dramatic than in the previous case.

Figure 4.6(b) shows that the energy evolution of the lattice initialized with an ordered state at $T = 2.4$ no longer begins at equilibrium, but follows a trend similar to the disordered case.

Figure 4.7(a) and Figure 4.7(b) shows, in principle, the total magnetization at $T = 2.4$ for a disordered and ordered initial state, respectively. Though, both figures are hard to interpret due to much noise in terms of fluctuations. This comes as no surprise considering that $T = 2.4$ which is greater than the expected Curie temperature where the magnetization disappears. The noise is thus presumably thermal noise.

All results considered, the implemented Metropolis algorithm seems to conserve both the tendency for a system to minimize its energy and ergodicity. The number of cycles needed to reach the most likely state are hard to interpret in the higher temperature cases, as there is much noise in terms of fluctuations.

5.4 Number of Accepted States

Figure 4.8 shows a linear relation between the number of accepted states and the number of Monte Carlo cycles. The first data sample is extracted after 1000 cycles, meaning that system will have reached the most likely state and fluctuates around this energy (if the tendency discussed in the previous section holds). The average number of accepted states will thus be constant in time.

Figure 4.9 shows that the number of accepted states per sweep as a function of temperature increases with the temperature. This behavior is consistent with the acceptance amplitude moving towards unity as the temperature increases, meaning that higher energy states will be more frequently accepted.

5.5 Probability Distribution

Figure 4.10(a) shows that the distribution at $T = 1$ is skewed heavily towards lower energy states, with the lowest possible energy state, $E_i = -800$, being the most likely state, by far. This corresponds with the discussion in Section 5.3.

Figure 4.10(b) shows that the distribution at $T = 2.4$ resembles a normal distribution, though it is somewhat skewed. More energy states are available to the system when the temperature increases, and the distribution is nearly centered around the most likely energy state $E_i \approx -480$.

These results correspond well with the expectation of more probable energy states at higher temperatures and that the most likely state is at a higher energy as the temperature increases.

The variance calculated from the specific heat capacity, computed in the same simulation, yielded

$$\sigma_E^2 = 9.216 \quad \text{for } T = 1$$

and

$$\sigma_E^2 = 3258 \quad \text{for } T = 2.4$$

These values seem to match the distributions well (after all, they originate from the same data), so the implementation seems to have been successful.

5.6 Studies of Phase Transitions

Figure 4.11 shows that the mean energy tends to increase as the temperature increases for several lattices of different size. This corresponds with the previous discussions. The figure does not give any information about a phase transition.

Figure 4.12, on the other hand, shows signs of a phase transition as the mean magnetization drops rapidly around the expected Curie temperature T_C . The drop is steeper for higher lattice sizes, in accordance with the expectation, that is, $\langle |\mathcal{M}| \rangle \rightarrow 0$ with an infinite slope for an infinitely large lattice at T_C . From the figure, it can be extracted that the mean magnetization drops more sharply in the temperature range $T \in [2.25, 2.30]$. Thus, it is implied that the simulated Curie temperature is confined within this range.

Figure 4.13 and Figure 4.14 clearly shows a maxima in the specific heat capacity and magnetic susceptibility, respectively, at a given temperature. In addition, the peak of these maximum values becomes sharper as the lattice size increases. This indicates the divergent behavior expected in the thermodynamic limit (infinitely large lattice).

5.7 Parallelization Speedup

Table 4.2 shows that the obtained speedup when moving from one (without parallelization) to eight threads (with parallelization) is about 5.56 times as fast in the simulation with $N = 10^5$ Monte Carlo cycles and zero precycles. In theory, a speedup closer to 8 times as fast could be expected. Though, a speedup exactly proportional to the number of threads is not really attainable since MPI is not 100% efficient.

Table 4.3 shows that the obtained speedup when moving from one (without parallelization) to eight threads (with parallelization) is about 4.98 times as fast in the simulation with $N = 10^5$ Monte Carlo cycles and 1000 precycles. This is a poorer speedup than in the previous case. When using precycles, each node spends time thermalizing the system. By invoking a strategy such as using the final configuration in the previous simulation as the initial configuration in the next when simulating consecutive temperatures, this problem could have been mostly avoided.

5.8 Extracting the Curie Temperature

From the linear regression in [Figure 4.15](#), found through the linear finite scaling relations given by [Equation \(2.21\)](#), the estimated Curie temperature at the thermodynamic limit was found to be

$$k_B T_C / J = 2.2676 \approx 2.268$$

The exact result, introduced with [Equation \(2.22\)](#), is

$$k_B T_C / J = \frac{2}{\ln(1 + \sqrt{2})} \approx 2.2692$$

The estimated value is thus correct to three digits, which seems reasonable considering that the resolution of the temperature was $\Delta T = 0.01$ in the simulation from which the fitted values were extracted. The result could have been made more accurate by increasing the resolution and simulating even larger lattices. However, this would have increased the simulation time significantly. All in all, the result found corresponds sufficiently well with the exact result.

6 Conclusion

In this project the square lattice Ising model for a magnetic system with ferromagnetic ordering was used to simulate phase transitions, with the aim to determine the Curie temperature T_C . The Metropolis algorithm was used to calculate the Ising model estimations. Benchmarking the implementation with analytical results for a 2×2 lattice yielded a good precision with $N = 10^7$ Monte Carlo cycles. A relative error of order 10^{-5} , 10^{-5} , 10^{-4} and 10^{-3} for the mean energy, absolute value of mean magnetization, specific heat capacity, and magnetic susceptibility, respectively, was obtained. The numerical precision was also conserved for temperatures in the range $T = 1$ to $T = 3$. In simulations with various finite lattices of size $L \times L$, specifically $L = 40, 60, 100, 160$, the Curie temperature was extracted with finite scaling relations as $k_B T_C / J \approx 2.268$. This corresponds well with the exact result, $k_B T_C / J = 2 / \ln(1 + \sqrt{2}) \approx 2.269$, provided by Onsager [\[1\]](#).

7 Future Work

The implementation of the code in this project can be optimized to some extent. The most striking possible optimization would be to add a better way of initializing the system to shorten the time it takes to reach equilibrium. As discussed in [Section 5.7](#), using the final configuration of the previous simulation as the initial configuration for the next when simulating consecutive temperatures could be a means to that end.

Furthermore, the class `Ising` could be extended to contain different physical systems, with the `Metropolis` class remaining mostly as is. A natural extension of the `Ising` class would be to add an external magnetic field to the model, so that phenomena such as magnetic hysteresis could be studied. Extending the model to include all three dimensions is also a possible continuation.

References

- [1] Lars Onsager. “Crystal Statistics. I. A Two-Dimensional Model with an Order-Disorder Transition”. In: *Phys. Rev.* 65 (3-4 Feb. 1944), pp. 117–149. DOI: [10.1103/PhysRev.65.117](https://doi.org/10.1103/PhysRev.65.117). URL: <https://link.aps.org/doi/10.1103/PhysRev.65.117> (cit. on pp. 7, 26).
- [2] Dysthe. D. K. Malthe-Sørenssen A. *Statistical and Thermal Physics Using Python*. Department of Physics, University of Oslo, 2017 (cit. on pp. 2–4, 8, 9).
- [3] M. H. Jensen. *Computational Physics – Lecture Notes Fall 2015*. Department of Physics, University of Oslo, 2015. URL: <https://github.com/CompPhysics/ComputationalPhysics/blob/master/doc/Lectures/lectures2015.pdf> (cit. on pp. 2–4, 6–10).
- [4] R. Nave. *Ferromagnetism*. URL: <http://hyperphysics.phy-astr.gsu.edu/hbase/Solids/ferro.html> (visited on 11/21/2018) (cit. on p. 4).